

CASTOR detector: Model, objectives and simulated performance^(*)^()**

A. L. S. ANGELIS⁽¹⁾, X. ASLANOGLU⁽²⁾, J. BARTKE⁽³⁾, M. YU. BOGOLYUBSKY⁽⁴⁾
K. CHILEEV⁽⁵⁾, S. ERINE⁽⁴⁾, E. GŁADYSZ-DZIADUŚ⁽³⁾, YU. V. KHARLOV⁽⁴⁾
A. B. KUREPIN⁽⁵⁾, M. LOBANOV⁽⁴⁾, A. I. MAEVSKAYA⁽⁵⁾
G. MAVROMANOLAKIS⁽¹⁾^(***), N. NICOLIS⁽²⁾, A. D. PANAGIOTOU⁽¹⁾
S. A. SADOVSKY⁽⁴⁾ and Z. WŁODARCZYK⁽⁶⁾

⁽¹⁾ Nuclear and Particle Physics Division, University of Athens - Athens, Greece

⁽²⁾ Department of Physics, University of Ioannina - Ioannina, Greece

⁽³⁾ Institute of Nuclear Physics - Cracow, Poland

⁽⁴⁾ Institute for High Energy Physics - Protvino, Russia

⁽⁵⁾ Institute for Nuclear Research - Moscow, Russia

⁽⁶⁾ Institute of Physics, Pedagogical University - Kielce, Poland

(ricevuto il 21 Ottobre 2000; approvato il 12 Febbraio 2001)

Summary. — We present a phenomenological model describing the formation and evolution of a Centauro fireball in the baryon-rich region in nucleus-nucleus interactions in the upper atmosphere and at the LHC. The small particle multiplicity and imbalance of electromagnetic and hadronic content characterizing a Centauro event and also the strongly penetrating particles (assumed to be strangelets) frequently accompanying them can be naturally explained. We describe the CASTOR calorimeter, a subdetector of the ALICE experiment dedicated to the search for Centauro in the very forward, baryon-rich region of central Pb+Pb collisions at the LHC. The basic characteristics and simulated performance of the calorimeter are presented.

PACS 12.38.Mh – Quark-gluon plasma.

PACS 25.75 – Relativistic heavy-ion collision.

PACS 96.40 – Cosmic rays.

PACS 01.30.Cc – Conference proceedings.

^(*) Paper presented at the Chacaltaya Meeting on Cosmic Ray Physics, La Paz, Bolivia, July 23-27, 2000.

^(**) Further CASTOR related information at <http://www.cern.ch/mavromag/castor>.

^(***) E-mail: gmavroma@mail.cern.ch.

1. – Introduction

Centauro events [1] exhibit relatively small particle multiplicity compared to normal hadronic events, complete absence or strong suppression of the electromagnetic component and very high $\langle p_t \rangle$. Furthermore, a number of hadron-rich events are accompanied by a strongly penetrating component observed in the form of halo, strongly penetrating clusters [2,3] or long-living cascades, whose transition curves exhibit a characteristic form with many maxima and slow attenuation [4,5]. These events have until now systematically defied all attempts at explanation in terms of conventional physics [6].

2. – Phenomenological model

According to a model we have developed, Centauro are considered to be the products of hadronization of a deconfined quark matter fireball formed in nucleus-nucleus collisions in the upper atmosphere [7-9]. The development of the fireball is summarized below.

Formation of a deconfined quark matter fireball

The deconfined quark matter (DQM) fireball is created in the baryon-rich projectile fragmentation region. Initially, it consists of u, d quarks and gluons. Due to the very high baryochemical potential ($\mu_b \gg m_N$), the creation of $u\bar{u}$ and $d\bar{d}$ quarks is highly suppressed (Pauli blocking of u, d quarks and the factor $\exp[-\mu_q/T]$ for antiquarks), resulting in the fragmentation of gluons into $s\bar{s}$ predominantly. This results in the suppressed production of pions, due to the absence of \bar{u} , \bar{d} , and hence to the suppression of photons.

Chemical equilibrium

A state of partial chemical equilibrium may be achieved in a time interval $\sim 10^{-23}$ s, the relaxation time for $g \rightarrow s\bar{s}$. During this time several $K^+(\bar{s}u)$ and $K^0(\bar{s}d)$ are emitted, carrying away strange antiquarks, positive charge, entropy and lowering further the temperature.

Strange quark-matter state

The initially quark-matter fireball (u, d mixture) is now a slightly strange quark-matter state (u, d and s mixture). The s quarks are unable to hadronize due to the absence of \bar{u} , \bar{d} . This results in the finite excess of strange quarks and their stabilizing effects may transform the fireball into a long-lived state, stable against strong interactions, with $\tau_{\text{centauro}}^0 > 10^{-13}$ s able to reach mountain-top altitudes [10].

Hadronization

A mechanism of strangeness separation [11] can cause the strange quark content of the fireball to form low-mass strangelets. The fireball finally decays into baryons and long-lived strangelet(s), which have a very high strangeness-to-baryon ratio ($f_s = N_s/A \sim 1$), very low charge-to-baryon ratio ($Z/A \leq 0$), and small mass ($A_{\text{str}} \sim 7-15$). Simulations [12,13] show that they could be identified as the highly penetrating particles frequently accompanying the hadron-rich cosmic ray events.

In this manner, both the basic characteristics of the Centauro events (small multiplicities and extreme imbalance of electromagnetic to hadronic content) and the strongly penetrating component are naturally explained.

In a similar way, Centauro events may be produced in Pb+Pb collisions at the LHC from the hadronization of a quark-gluon plasma state formed in the beam fragmentation region, where the baryon number is expected to be strongly concentrated [8,14]. In table I

TABLE I. – Average characteristic quantities of modeled Centauro events and strangelets produced in cosmic rays and expected at the LHC.

Centauro event	Cosmic rays	LHC
Interaction	Fe+N	Pb+Pb
\sqrt{s} per nucleon	> 6.8 TeV	5.5 TeV
Fireball mass	> 180 GeV	~ 500 GeV
Projectile rapidity(y_{proj})	≥ 11	8.67
Lorentz factor γ	10^4	$\simeq 300$
Centauro pseudorapidity(η_{cent})	9.9	$\simeq 5.6$
$\Delta\eta_{\text{cent}}$	1	$\simeq 0.8$
$\langle p_T \rangle$	1.75 GeV	1.75 GeV (*)
Lifetime	10^{-9} s	10^{-9} s (*)
Decay probability	10% ($x \geq 10$ km)	1% ($x \leq 1$ m)
Strangeness	14	60–80
f_s (S/A)	$\simeq 0.2$	0.30–0.45
Z/A	$\simeq 0.4$	$\simeq 0.3$
Event rate	$\simeq 1\%$	$\sim 500/\text{month}$
“Strangelet”	Cosmic rays	LHC
Mass	$\sim 7\text{--}15$ GeV	10–80 GeV
Z	$\lesssim 0$	$\lesssim 0$
f_s	$\simeq 1$	$\simeq 1$

(*) Assumed.

we compare characteristic quantities of Centauro and strongly penetrating components (strangelets), either experimentally observed or calculated within the context of our model, for cosmic ray interactions and for Pb+Pb collisions at the LHC.

3. – The CASTOR detector in ALICE

Based on the above model, we have designed the CASTOR (Centauro And STRange Object Research) subdetector [14, 15] of the ALICE heavy ion experiment [16] at the LHC, in order to study the very forward, baryon-dense phase space region.

The CASTOR detector is a Cherenkov-effect-based calorimeter with tungsten absorber and quartz fibers as active material. The signal, namely the Cherenkov light

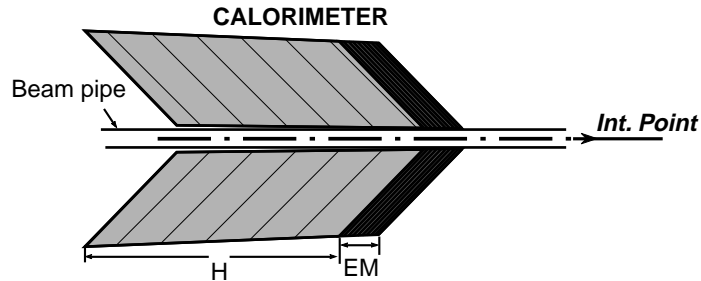


Fig. 1. – Schematic representation of a side view of the CASTOR calorimeter.

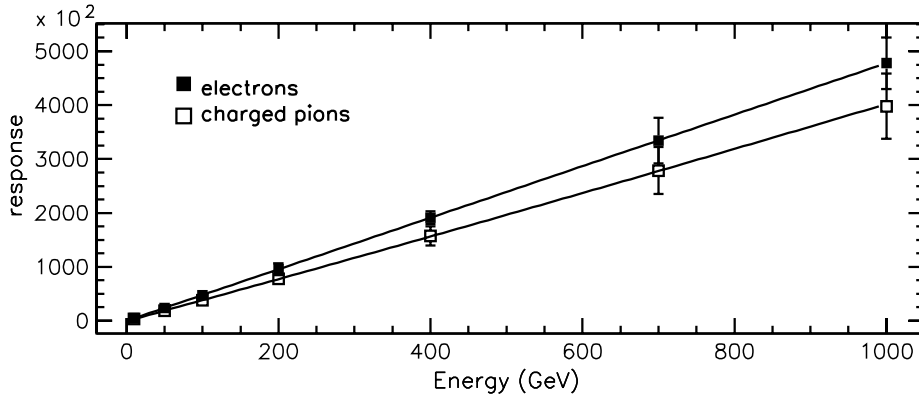


Fig. 2. – Simulated response (Cherenkov photons) to electrons and charged pions *vs.* incident particle energy.

produced by the shower charged particles traversing the fibers, will be collected and transmitted to PMTs through aircore lightguides. The W absorber quartz fiber planes sandwiches are inclined at 45° with respect to the beam axis to achieve maximum light production. The calorimeter is azimuthally divided into 8 octants and longitudinally segmented into layers (fig. 1). Each absorber layer is followed by a number of quartz-fiber planes. The detector will be placed at 16.4 m from the interaction point covering the pseudorapidity range $5.46 \leq \eta \leq 7.14$. Its main objective is to search in the baryon rich, very forward rapidity region of central Pb+Pb collisions for Centauro events and “strongly penetrating objects” by measuring the hadronic and electromagnetic energies and the hadronic showers’ longitudinal profile. It will work in an event-by-event mode and will complement the physics program pursued by the rest of the ALICE experiment essentially in the baryon-free midrapidity region.

4. – Simulated performance of the CASTOR calorimeter

Detailed simulation studies of the performance of the CASTOR calorimeter have been done [17, 18]. The calorimeter shows linear response to electrons and hadrons,

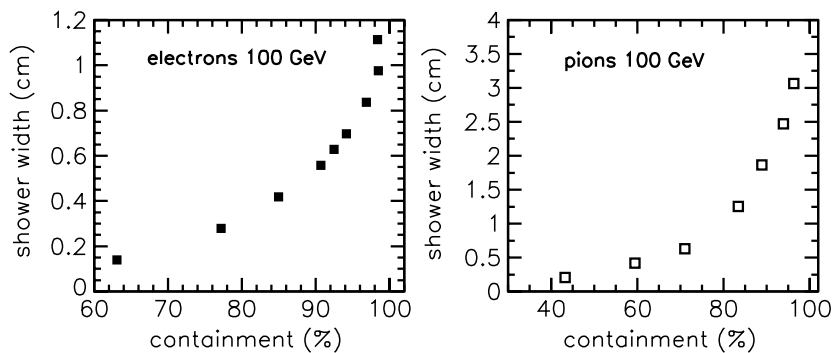


Fig. 3. – Electron and charged pion shower transverse width *vs.* signal containment.

satisfactory energy resolution and very narrow visible transverse size of electromagnetic and hadronic showers. The results presented here refer to a configuration in which each octant is longitudinally segmented into 200 layers of 3 mm thick W absorber followed by 2 planes of fibers. The fiber has quartz core (diameter 0.60 mm), silicone cladding (diameter 0.64 mm) and numerical aperture 0.40. The layers are inclined by 45° relative to the beam axis, resulting in a total calorimeter depth of $9.2 \lambda_I$.

Figure 2 shows the total number of Cherenkov photons produced and captured inside the fibers as a function of the energy of incident electrons and charged pions. We expect a response of about 478 and 385 photons per GeV for incident electrons and charged pions, respectively. Figure 3 shows the shower transverse width *versus* signal containment for 100 GeV incident electrons and charged pions. We obtain a visible shower transverse width of 0.7 cm and 2.7 cm, respectively, for 95% signal containment. Narrow visible shower size is a common feature of quartz fiber calorimeters and derives from their operation principle, based on the Cherenkov effect, making them sensitive essentially only to the shower core [19, 20].

The propagation of strangelets inside the CASTOR calorimeter has also been simulated, as described in [12, 21]. The study of such simulated events shows that the expected signal can be easily distinguished from the hadronic background for strangelets with energy ≥ 20 TeV. Sophisticated methods based on neural-network techniques for pattern recognition are also being developed [22] in order to achieve high efficiency in the detection of low energy strangelets as well. The neural-network classification method seems to significantly improve the experimental signal-to-background ratio (in the raw data recorded) by a large factor resulting in a subset of data to be analyzed with a signal-to-background ratio in the range of 0.1 to 1 or higher. A factor of signal-to-background improvement of the order of 1000 or higher can be achieved for neural-network's signal classification efficiency at about 96%.

REFERENCES

- [1] LATES C. M. G., FUGIMITO Y. and HASEGAWA S., *Phys. Rep.*, **65** (1980) 151.
- [2] HASEGAWA S. and TAMADA M., *Nucl. Phys. B*, **474** (1996) 225.
- [3] BARADZEI L. T. *et al.*, *Nucl. Phys. B*, **370** (1992) 365.
- [4] ARISAWA T. *et al.*, *Nucl. Phys. B*, **424** (1994) 241.
- [5] BUJA Z. *et al.*, *Proceedings of the 17th ICRC (Paris)*, vol. **11** (1981) p. 104.
- [6] TAMADA M., Inst. Cosmic Ray Research, Univ. Tokyo ICRR-Report-454-99-12.
- [7] ASPROULI M. N., PANAGIOTOU A.D. and GLADYSZ-DZIADUS E., *Astropart. Phys.*, **2** (1994) 167.
- [8] PANAGIOTOU A. D., PETRIDIS A. and VASSILIOU M., *Phys. Rev. D*, **45** (1992) 3134.
- [9] PANAGIOTOU A. D., KARABARBOUNIS A. and PETRIDIS A., *Z. Phys. A*, **333** (1989) 355.
- [10] THEODORATOU O. P. and PANAGIOTOU A. D., *Astropart. Phys.*, **13** (2000) 173.
- [11] GREINER C. *et al.*, *Phys. Rev. D*, **38** (1988) 2797.
- [12] GLADYSZ-DZIADUS E. and WLODARCZYK Z., *J. Phys. G*, **23** (1997) 2057.
- [13] GLADYSZ-DZIADUS E. and PANAGIOTOU A. D., *Proc. Int. Symp. on Strangeness & Quark Matter*, edited by G. VASSILIADIS *et al.* (World Scientific, Singapore) 1995, p. 265.
- [14] A. L. S. ANGELIS *et al.*, hep-ex/9901038 and in *Proceedings of the XXVIII International Symposium on Multiparticle Dynamics, Delphi, Greece, Sept. 1998*, edited by N. G. ANTONIOU *et al.* (World Scientific, Singapore) 1999, pp. 134-142.
- [15] ANGELIS A. L. S. *et al.*, CASTOR proposal, Internal note ALICE/CAS 97-07.
- [16] ALICE COLLABORATION, Technical Proposal, CERN/LHCC/95-71.

- [17] MAVROMANOLAKIS G., ANGELIS A. L. S. and PANAGIOTOU A.D., Internal note ALICE/CAS 2000-20.
- [18] MAVROMANOLAKIS G., ANGELIS A. L. S. and PANAGIOTOU A.D., Internal note ALICE/CAS 2000-25.
- [19] BRITZ J. *et al.*, RD40 Project, CERN/LHCC 95-27.
- [20] GORODETZKY P. *et al.*, *Nucl. Instrum. Methods A*, **361** (1995) 161.
- [21] ANGELIS A. L. S., BARTKE J., GLADYSZ-DZIADUS E. and WLODARCZYK Z., *EPJ direct C*, **9** (1999) 1, DOI 10.1007/s1010599c0009.
- [22] MAVROMANOLAKIS G., preprint UA-NPPS/9/2000, work in preparation.